РАДІОФІЗИКА

РАДИОФИЗИКА

RADIOPHYSICS

UDC 539.2

Babich A. V.[1], Pogosov V. V.[2], Vakula P. V.[3]

[1]Ph.D in solid state physics, docent, Zaporizhian National Technical University, Ukraine
[2]Doctor of science (mathematical and physic), professor, Zaporizhian National Technical University, Ukraine
[3]Assistant, Zaporizhian National Technical University, Ukraine, E-mail: vakulapavel@gmail.com.

SELF-CONSISTENT CALCULATIONS OF WORK FUNCTION, SHOTTKY BARRIER HEIGHTS AND SURFACE ENERGY OF METAL NANOFILMS IN DIELECTRIC CONFINEMENT

We suggest a method for the self-consistent calculations of characteristics of metal films in dielectric environment. Within a modified Kohn-Sham method and stabilized jellium model, the most interesting case of asymmetric metal-dielectric sandwiches is considered, for which dielectric media are different from the two sides of the film. As an example, we focus on Na, Al and Pb. We calculate the spectrum, electron work function, and surface energy of polycrystalline and crystalline films placed into passive isolators. We find that a dielectric environment generally leads to the decrease of both the electron work function and surface energy. It is revealed that the change of the work function is determined only by the average of dielectric constants from both sides of the film. We introduced the position of a conductivity band in the dielectric as a parameter in the self-consistency procedure and performed calculations, using image potential, for the aluminum film with ideal interfaces vacuum/Al(111)/SiO_2, vacuum/Al(111)/AlO and sandwiches SiO/Al(111)/AlO. As a result, effective potential profiles and the Schottky barrier heights were calculated.

Keywords: metal nanofilm, dielectric, work function, surface energy, Schottky barrier height.

1. INTRODUCTION

Thin metal films and flat islands on semiconductor or dielectric substrates can be considered as two-dimensional electron systems with properties, which are of interest both from the fundamental point of view and from the perspective of their application in nanoscale electronic devices.

There are a limited number of experimental works focused on quantum size effects in such systems (for reviews, see [1–9]) due to difficulties in sample fabrication, as well as because of lack of suitable experimental methods. One of the most important characteristics of metal nanostructures is electron work function.

As a rule, calculations of electron work functions for films are performed for the idealized case of films in vacuum. Similarly to clusters, this quantity defines an ionization potential. There are different methods, which enable one to calculate electron structure of slabs (in vacuum) consisting of few monoatomic layers (ML). Let us combine them into three groups according to the complexity of computations: I – the Sommerfeld electrons in-a-box model (analytical calculations, slabs and wires) [10–15]; II – self-consistent calculations within various versions of jellium model (slabs and wires) [16–20]; III – *ab initio* calculations (slabs) [21–24]. The obtained results are illustrated in Fig. 1 for all these three groups. An important ingredient of approaches within group III is the monolayer number in the film (see dots in Fig. 1). For groups I and II, L changes continuously.

In group I, the Fermi energy (kinetic energy) $\varepsilon_F(L)$ is counted from the *flat* bottom of conductivity band, while the work function $W(L)$ is counted from the vacuum level. Therefore, their size dependencies are «asymmetric». In addition to quantum oscillations, these quantities contain monotonic size contributions, which, at small film thicknesses, *together* show up through inequalities $0 < W(L) < W_0$ and $\varepsilon_F(L) > \overline{\varepsilon}_F > 0$, where W_0 and $\overline{\varepsilon}_F$ correspond to the three dimensional (3D) metal (allowing for the energy counting for $\overline{\varepsilon}_F$).

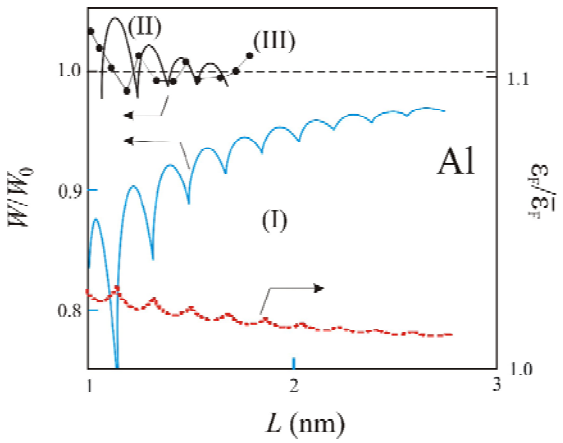

Fig. 1. Illustration of the computation results for groups I, II and III (data for group I are deduced from [12])

In [25, 26], an asymptotic behavior of electron chemical potential for spherical clusters of radius R was determined, from which it follows that

$$W(R) = W_0 - \frac{c_1}{R} < W_0, \qquad (1)$$

where $c_1 = 2,5eV \cdot a_0$ for simple metals, $a_0 = \hbar^2/(me^2)$. It is expectable that such a monotonic contribution must appear for films also. However, in contrast to the case of group I, self-consistent calculations of groups II and III (see Fig. 1), at small film thickness, point out to the suppression of monotonic dependence (having an asymptotic (1)) by corrections of higher orders of smallness. For instance, compensation of terms $-c_1/L + c_2/L^2$ occurs at $L^* = c_2/c_1$, and L^* is large, provided $c_2 >> c_1 > 0$.

Experimental results also do not allow to draw unambiguous conclusions on the character of monotonic component of $W(L)$: in experiments [3], it is absent (Yb films on Si substrate), while, according to [2, 5], it coincides with the one of group I. Note that the comparison of a measured work function for the sandwich consisting of Ag film on Fe(100) in [2, 5] with calculated results for slabs *in vacuum* is rather relative.

If the film placed on the substrate is considered, in order to determine characteristics of contacts in the easiest case, it is necessary to know the dielectric constant κ as well as the position of conductivity band $-\chi$ (χ is the electron affinity) in dielectric material. The approximation $\chi = 0$ was widely used to the work function, polarizability and surface plasmon resonance of jellium spheres and wires embedded in different dielectric matrices (see [19, 27–29] and references therein).

The aim of this work is to compute energy characteristics of metal films in dielectrics. We suggest a method for self-consistent calculations of equilibrium profiles of electron concentration, effective potential, energy spectrum, and integral characteristics of metal films in dielectrics and dielectric substrates. The developed method is based on a stabilized jellium model [30] and lcal density approximation for exchange-correlation potential [31], which were used by us before [32] to analyze characteristics of semi-infinite metal with dielectric coating. For our problem, in the spirit of Serena et al. [33], we introduce the nonlocal potential matched at the image-plane positions to the local exchange-correlation potential. We also introduce the position of a conductivity band in the dielectric as a parameter in the self-consistency procedure and performed calculations the effective potential profiles and the Schottky barrier heights for the vacuum/$Al(111)/SiO_2$, vacuum/$Al(111)/Al_2O_3$ and sandwich $SiO_2/Al(111)/Al_2O_3$.

This paper is organized as follows. In Section II, we formulate our model. In Section III, we presents our main results and provide a discussion of them. We conclude in Section IV.

2. MODEL

Let us consider a metallic film of thickness L at zero temperature. We direct z-axis perpendicularly to the film surface (Fig. 2 (*a*), $\Lambda >> L$).

Principal identities for the film can be obtained within a model of a rectangular well for conduction electrons. To perform a preliminary analysis, we suppose that the bottom of the potential well is flat and we count energies starting from its value. Final expression for the kinetic energies of conduction electrons depends only on energy differences; therefore, energies counting in such a way is allowed.

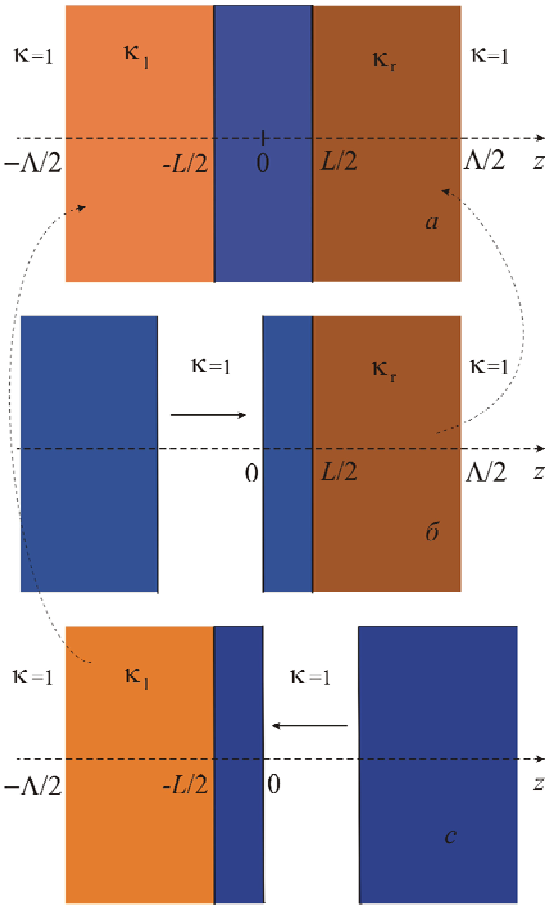

Fig. 2. (*a*) – Scheme of the film in dielectric environment; (*b*) and (*c*) – split semi-infinite metal samples, which have been in contact with dielectrics before the splitting. Split parts form a sandwich in figure 2 (*a*)

We study a film of thickness L comparable in magnitude to the Fermi wavelength $\bar{\lambda}_F = 2\pi / \bar{k}_F$ of an electron in 3D metal. The longitudinal sizes of the sample are assumed to be considerably larger than the film thickness ($L = L_x, L_y$), which leads to the pronounced quantization of the transverse component of the electron momentum. The three-dimensional Schrodinger equation for a quantum box can be separated into one-dimensional equations.

The eigenenergies are given by

$$\varepsilon_{ik_\parallel} = \varepsilon_i + \frac{k_\parallel^2}{2}, k_\parallel^2 = k_x^2 + k_y^2, \qquad (2)$$

where ε_i is the eigenvalue of the i-th perpendicular state $\psi_i(z)$ (hereafter the Hartree atomic units are used: $\hbar = m = e = 1$). The eigenvalue ε_i is the bottom of the i-th subband. For finite and periodic systems in the z-direction Dirichlet and periodic boundary conditions are used, respectively. Therefore, possible allowed electron states k_x, k_y, k_z form a system of parallel planes in the k-space, $k_z \equiv k_i$.

Occupation of electron states starts from the point $\{0,0,k_1\}$ and follows an increase of radius-vector. As a result, it turns out that all the occupied states are contained within the area of k-space, confined between the plane $k_z = k_1$ and semi-sphere of radius $k_F = \sqrt{2\varepsilon_F}$ (see Fig. 3).

The number of states dZ in each of the circles, formed by the intersection of Fermi semi-sphere with planes $k_z = k_i$ of area $S = L_x L_y$, within the interval of wave vectors $(k_\parallel, k_\parallel + dk_\parallel)$ and taking into account both possible spin projections, is $dZ(k_\parallel) = 2Sd(\pi k_\parallel^2)/(2\pi)^2$. The maximum value of $k_\parallel$ in each circle numbered by i, is equal to the circle radius $k_{F(i)} = (k_F^2 - k_i^2)^{1/2}$. In order to find the number of the occupied states, which coincides with the number of valence electrons N in the film, one should integrate dZ over $k_\parallel$ in each circle, and then sum up contributions of all the circles:

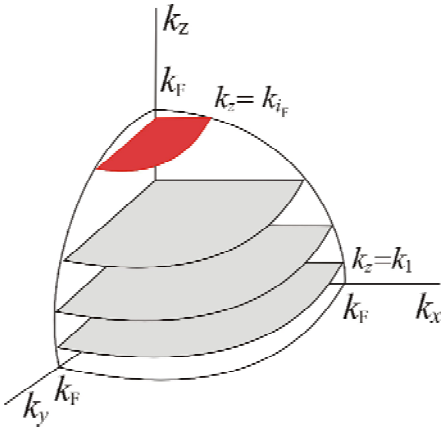

Fig. 3. Scheme for the occupation of electronic states in the k space

$$N = \frac{S}{\pi}\sum_{i=1}^{i_F}\int_0^{k_{F(i)}} dk_\parallel k_\parallel = \frac{S}{2\pi}\left(i_F k_F^2 - \sum_{i=1}^{i_F} k_i^2\right). \qquad (3)$$

Taking into account an expression for electron kinetic energy $\frac{1}{2}(k_\parallel^2 + k_i^2)$, the total kinetic energy of electron subsystem equals

$$T_s = \frac{S}{2\pi}\sum_{i=1}^{i_F}\int_0^{k_{F(i)}} dk_\parallel k_\parallel \left(k_\parallel^2 + k_i^2\right) = \frac{S}{4\pi}\sum_{i=1}^{i_F} k_{F(i)}^2\left(\frac{k_{F(i)}^2}{2} + k_i^2\right), \qquad (4)$$

where i_F is the number of the last occupied or partially occupied subband.

In the frame of density-functional theory and stabilized jellium model (SJ), the total energy of metal sample is represented by the functional of nonhomogeneous electron concentration $n(r)$:

$$E_{SJ}[n(r)] = T_s + E_{xc} + E_H + E_{ps} + E_M, \qquad (5)$$

where T_s is the (non-interacting) electron kinetic energy, E_{xc} is the exchange-correlation energy, E_H is the Hartree (electrostatic) energy, E_{ps} is the pseudopotential (Ashcroft) correction, and E_M is the Madelung energy. The sum of first three terms in expression (5) corresponds to the energy of «ordinary» jellium, E_J. The average energy per valence electron in the bulk of metal is $\bar{\varepsilon}_{SJ,J} = E_{SJ,J}[\bar{n}]/N$, where N is a total number of free electrons of concentration $\bar{n}$, defined by valence and atomic density.

The positive (ionic) charge distribution can be modeled by the step function

$$\rho(z) = \bar{n}\theta(L/2 - |z|). \qquad (6)$$

Solving the Kohn-Sham equations

$$-\frac{1}{2}\nabla^2\psi_i(z) + v_{eff}\left[z, n(z)\right]\psi_i(z) = \varepsilon_i\psi_i(z), \qquad (7)$$

$$v_{eff}[z, n(z)] = \phi(z) + v_{xc}(z) + \langle\delta v\rangle_{face}\,\theta(L/2 - |z|) \qquad (8)$$

together with the Poisson equation

$$\nabla^2\phi(z) = -\frac{4\pi}{\kappa(z)}\left[n(z) - \rho(z)\right], \qquad (9)$$

with the step function

$$\kappa(z) = \begin{cases} 1; & z < -\Lambda/2, -L/2 < z < L/2, z > \Lambda/2, \\ \kappa_1; & -\Lambda/2 < z < -L/2, \\ \kappa_r; & L/2 < z < \Lambda/2, \end{cases} \qquad (10)$$

we obtain the single electron wave function and the eigenvalue ε_i self-consistently.

It is generally believed that the more «physical» potential, the better the result of computations for the location of the Fermi energy (as the eigenvalue of the highest occupied state). One of the limitations of the method of effective potentials in LDA is its failure in reproducing a correct behavior of image potentials outside metal surfaces (see [34] and references therein). Therefore, for our problem, in the spirit of the work [33], we introduce the nonlocal potential $v_{xc}^{\mathrm{NL}}(z)$ matched at the image-plane positions to the local exchange-correlation potential $v_{xc}^{\mathrm{LD}}(z) = d[n(z)\varepsilon_{xc}(z)]/dn(z)$:

$$v_{\mathrm{xc}}(z) = \begin{cases} v_{xc}^{\mathrm{NL,l}}(z), & z \le Z^{\mathrm{l}}, \\ v_{xc}^{\mathrm{LD}}(z), & Z^{\mathrm{l}} \le z \le Z^{\mathrm{r}}, \\ v_{xc}^{\mathrm{NL,r}}(z), & z \ge Z^{\mathrm{r}}, \end{cases} \tag{11}$$

where $Z^{\mathrm{l}} = -L/2 - z_0^{\mathrm{l}}$, $Z^{\mathrm{r}} = L/2 + z_0^{\mathrm{r}}$, and the image-plane positions ($z_0^{\mathrm{l,r}} > 0$) are counted from the left and right sides of film surfaces,

$$v_{xc}^{\mathrm{NL,l}} = -\chi^{\mathrm{l}} + \frac{1-[1-(z-Z^{\mathrm{l}})/(4\lambda_{\mathrm{l}})]e^{(z-Z^{\mathrm{l}})/\lambda_{\mathrm{l}}}}{4\kappa_{\mathrm{l}}(z-Z^{\mathrm{l}})}, \tag{12}$$

$$v_{xc}^{\mathrm{NL,r}} = -\chi^{\mathrm{r}} - \frac{1-[1+(z-Z^{\mathrm{r}})/(4\lambda_{\mathrm{r}})]e^{-(z-Z^{\mathrm{r}})/\lambda_{\mathrm{r}}}}{4\kappa_{\mathrm{r}}(z-Z^{\mathrm{r}})}. \tag{13}$$

For instance, far from the surface, (13) has a correct asymptotic behavior $\{-\chi^{\mathrm{r}} - [4\varepsilon_{\mathrm{r}}(z-Z^{\mathrm{r}})]^{-1}\}$, which is an image potential. From the condition of matching of potential (11) as well as its first derivatives in the image planes from left and right sides, we obtain simple relations:

$$\lambda_{\mathrm{l,r}} = -\frac{3}{16\kappa_{\mathrm{l,r}}[v_{xc}^{\mathrm{LD}}(Z^{\mathrm{l,r}}) + \chi^{\mathrm{l,r}}]},$$

$$\frac{|\,dv_{xc}^{\mathrm{LD}}(z)/dz\,|_{z=Z^{\mathrm{l,r}}}}{[v_{xc}^{\mathrm{LD}}(Z^{\mathrm{l,r}}) + \chi^{\mathrm{l,r}}]^2} = \frac{16}{9}\kappa_{\mathrm{l,r}}. \tag{14}$$

The second relation in (14) is treated as an equation for $z_0^{\mathrm{l},r}$. The values of at the left and right sides out of the film are calculated self-consistently by solving at every iteration the Kohn-Sham equations. In this way the effective potential is matched self-consistently to its image-potential-like form at large distances. The result of the work [33] for the semi-infinite metal is reproduced $\kappa = 1$ and $\chi = 0$.

The term $\langle \delta \mathrm{v} \rangle_{face}$ in (8), which makes it possible to distinguish different crystal faces, represents the difference between the potential of the ionic lattice and the electrostatic potential of the positively charged background averaged over the Wigner-Seitz cell:

$$\langle \delta \mathrm{v} \rangle_{face} = \langle \delta \mathrm{v} \rangle_{WS} - \left(\frac{\bar{\varepsilon}_{\mathrm{M}}}{3} + \frac{\pi \bar{n}}{6} d^2 \right), \quad \langle \delta \mathrm{v} \rangle_{WS} = -\bar{n} \frac{d\varepsilon_{\mathrm{J}}}{d\bar{n}},$$

where d is the distance between the atomic planes parallel to the surface. The term $\langle \delta \mathrm{v} \rangle_{WS}$ describes a polycrystalline sample [30]. In equation (10) ε_{l} and ε_{r} are dielectric constants of isolators from the left and right side of the film, respectively.

The electron density profile $n(z)$ is expressed through the wave functions $\psi_i(z)$

$$n(z) = \frac{1}{2\pi} \sum_{i=1}^{i_{\mathrm{F}}} k_{\mathrm{F}(i)}^2 \frac{|\psi_i(z)|^2}{\int_{-\infty}^{+\infty} dz\,|\psi_i(z)|^2}. \tag{15}$$

Values of i_{F} and ε_{F} are determined by the solution of the equation

$$\pi L \bar{n} + \sum_{i=1}^{i_{\mathrm{F}}} \varepsilon_i - i_{\mathrm{F}} \varepsilon_{\mathrm{F}} = 0; \quad i = 1,2,\ldots,i_{\mathrm{F}}; \quad \varepsilon_i \le \varepsilon_{\mathrm{F}}, \tag{16}$$

which follows from the normalization condition (3) and definition of the Fermi energy. In this equation, the integration over $k_{\parallel}$ is already performed and therefore the summation is made only over the subband number.

In nanofilms, the spatial oscillation of a electronic density is significant throughout the sample. Therefore, energies are counted from the vacuum level, which is the energy of the electron in rest in the area $|z| >> \Lambda/2$. For bound states, energies are negative, including ε_{F}.

We use iterative procedure (see Appendix) allowing us to solve self-consistently the system of equations (7), (9), (15) and to find optimal profiles $n(z)$, $\varphi(z)$, as well as spectrum of one-particle energies. As a result, metal/vacuum and metal/dielectric work functions are defined in the form

$$W = -\varepsilon_{\mathrm{F}}, \tag{17}$$

$$W_{\mathrm{d}}^{\mathrm{l,r}} = -\varepsilon_{\mathrm{F}}(\kappa, \chi^{\mathrm{l,r}}) - \chi^{\mathrm{l,r}}. \tag{18}$$

There are two situations, when $|\varepsilon_{\mathrm{F}}| > \chi^{\mathrm{l,r}}$ and $\le \chi^{\mathrm{l,r}}$. The value W_{d} is the Schottky barrier height.

Let us consider a scheme for the surface energy determination (see figure 2 (*b*) and (*c*)) for the film of thickness L in a dielectric environment.

First, we take a semi-infinite metal (Me_{∞}) covered by a dielectric (κ_{r}). Let us denote the energy of such a sample as $E\{\mathrm{Me}_{\infty} \mid \kappa_{\mathrm{r}}\}$. We now split the sample and move the parts, as shown in Fig. 2 (*b*). As a result, two new surfaces of the same area S are formed, which are in a contact with the vacuum ($\kappa = 1$). We denote the energies of these two parts as $E\{\mathrm{Me}_{\infty} \mid 1\}$ and $E\{1 \mid \mathrm{Me}_{L/2} \mid \kappa_{\mathrm{r}}\}$, while the irreversible work A, which is needed to form them, as

$$E\{\mathrm{Me}_{\infty} \mid 1\} + E\{1 \mid \mathrm{Me}_{L/2} \mid \kappa_{\mathrm{r}}\} - E\{\mathrm{Me}_{\infty} \mid \kappa_{\mathrm{r}}\}. \tag{19}$$

Let us stress that, as a result of these manipulations, the «fabricated» sandwich represents a film of thickness $L/2 \geq d$ on the dielectric substrate in vacuum (air).

Similar manipulations with another sample (Fig. 2 (c)) require a work

$$E\{1\,|\,\mathrm{Me}_\infty\} + E\{\kappa_1\,|\,\mathrm{Me}_{L/2}\,|1\} - E\{\kappa_1\,|\,\mathrm{Me}_\infty\}. \quad (20)$$

Next, a simplifying step is taken in separating the total energy of the system into bulk and surface contributions, assuming that the former is the same for a thin film as for a semi-infinite film (see, for example, [18])

$$E = E^{\mathrm{b}} + E^{\mathrm{s}}.$$

Then, bulk components E^{b} do compensate in the expressions (19) and (20). In each case considered above, the specific surface energy γ equals $A/2S$. When the width of the film tends to infinity, the term E^{s} for the slab approaches the surface components of the semi-infinite system.

The work needed to «create» a film on a dielectric is

$$A\{\kappa\,|\,\mathrm{Me}_{L/2}\,|1\} = \frac{1}{2}[E^{\mathrm{s}}\{\kappa\,|\,\mathrm{Me}_{L/2}\,|1\} +$$

$$+ E^{\mathrm{s}}\{1\,|\,\mathrm{Me}_\infty\} - E^{\mathrm{s}}\{\kappa\,|\,\mathrm{Me}_\infty\}]. \quad (21)$$

Now, we join two sandwiches by their free surfaces. We obtain a film shown in Fig. 2 (*a*). The work to create it can be represented as the energy of *adhesion* of such two pieces with the minus sign

$$A\{\kappa_1\,|\,\mathrm{Me}_L\,|\,\kappa_{\mathrm{r}}\} = \frac{1}{2}[E^{\mathrm{s}}\{\kappa_1\,|\,\mathrm{Me}_L\,|\,\kappa_{\mathrm{r}}\} -$$

$$- E^{\mathrm{s}}\{\kappa_1\,|\,\mathrm{Me}_{L/2}\,|1\} - E^{\mathrm{s}}\{1\,|\,\mathrm{Me}_{L/2}\,|\,\kappa_{\mathrm{r}}\}]. \quad (22)$$

Electron density profiles and potentials for each of the contributions in the expressions (21) and (22) are different, so that they must be calculated self-consistently and separately.

As similar to the definition for the semi-infinite metal [35, 32], E^{s} for the film is determined by the difference between the total film energy (5) and the energy of homogeneous metal (stabilized jellium) of the same volume:

$$E^{\mathrm{s}}\{\kappa_1\,|\,\mathrm{Me}_L\,|\,\kappa_{\mathrm{r}}\} = E_{\mathrm{SJ}}(L) - SL\bar{n}\bar{\varepsilon}_{\mathrm{SJ}} =$$

$$= 2S\left\{\gamma_{\mathrm{J}} + \langle\delta\mathrm{v}\rangle_{\mathrm{face}} \int_{-L/2}^{L/2} dz[n(z) - \bar{n}]\right\}. \quad (23)$$

By using equation (4), quantum-mechanical definition of an energy

$$k_i^2 = -\int_{-\infty}^{\infty} dz\psi_i(z)\nabla^2\psi_i(z),$$

as well as the definition given by equation (23), we obtain an expression for the first component of γ_{J}:

$$\gamma_{\mathrm{s}} = \frac{1}{8\pi}\sum_{i=1}^{i_{\mathrm{F}}} k_{\mathrm{F}(i)}^2\left(\frac{1}{2}k_{\mathrm{F}(i)}^2 - \int_{-\infty}^{\infty} dz\psi_i(z)\nabla^2\psi_i(z)\right) - \frac{1}{2}L\bar{n}\bar{t}_{\mathrm{s}}, \quad (24)$$

where $\bar{t}_{\mathrm{s}} = 3\bar{k}_{\mathrm{F}}^2/10$ is the kinetic energy per 1 electron for bulk. The remaining components are

$$\gamma_{xc} = \frac{1}{2}\int_{-\infty}^{\infty} dzn(z)\varepsilon_{xc}[n(z)] - \frac{1}{2}L\bar{n}\varepsilon_{xc}(\bar{n}); \quad (25)$$

$$\gamma_{\mathrm{H}} = \frac{1}{4}\int_{-\infty}^{\infty} dz\varphi(z)\big[n(z) - \rho(z)\big]. \quad (26)$$

For asymmetric sandwiches, $\{\kappa_1\,|\,\mathrm{Me}_L\,|\,\kappa_{\mathrm{r}}\}$, due to the formal division on the doubled area, the surface energy is calculated «in average». This is the consequence of the definition of γ through the integral of tangential component of pressure tensor over z from $-\infty$ to $+\infty$. The pressure tensor contains the nonelectrostatic part and the Maxwell stress tensor (see, for example, [36]).

3. RESULTS AND DISCUSSION

We perform calculations for both polycrystalline and crystalline films made of Na, Al and Pb, with electron concentration $\bar{n} = 3/4\pi r_s^3$ with corresponding electron parameter $r_s = 3,99; 2,07$ and $2,30\,a_0$. The minimal thickness of «crystalline» sandwiches should be not less than $2d$. It must be equal to $4d$ for $\{\varepsilon_1\,|\,\mathrm{Me}\,|\,\varepsilon_{\mathrm{r}}\}$, only in the case Eq. (22) is used. d is comparable to $\bar{\lambda}_{\mathrm{F}}/2$ ($\bar{\lambda}_{\mathrm{F}} = 13,06$, $6,78$ and $7,53$ for Na, Al and Pb, respectively).

Let us firstly perform calculations: (i) taking into account formulas (11)–(14), in which it is formally assumed that $\chi = 0$ and $v_{xc} \equiv v_{xc}^{\mathrm{LD}}$; (ii) using (11)–(14) and $\chi \neq 0$.

(i) For symmetric sandwich the effect of a dielectric coating on the surfaces is reduced to the «elongation» of the electron distribution tail and the effective potential beyond the surface of a metal (polycrystalline films $\{1\,|\,\mathrm{Al}\,|1\}$ and $\{3\,|\,\mathrm{Al}\,|\,3\}$ on Fig. 4). The calculations were performed for $\kappa = 1,\ldots,12$. Inside the film one can see the Friedel oscillations of electron density with peaks near geometrical boundaries. The period of oscillations is close to $\bar{\lambda}_{\mathrm{F}}/2$ and only weakly depends on the presence of dielectric coatings. The situation is similar for Na and Pb films.

At the boundaries between the metal film and the coatings, there are jumps in the derivative of the electrostatic potential $\phi'(z)$, which disappear, provided the dielectric constants of the coatings are equal to 1. These jumps are due to the boundary conditions (28) at $z = \pm L/2$. The jumps are also reflected on $v_{\mathrm{eff}}(z)$ profile, since $\phi(z)$ is one of its components. In addition, at the borders, there are another jumps of not only the derivative $v_{\mathrm{eff}}'(z)$, but also of $v_{\mathrm{eff}}(z)$

profile itself for any values of κ, including $\kappa = 1$. Such jumps have another origin compared to the first ones. This fact is linked to some features of the model [30], namely to the presence of the effective potential component $\langle \delta v \rangle_{\text{face}} \theta(L/2 - |z|)$. These nonphysical jumps should not be taken into account in the estimation of the effective force

$$F_{\text{eff}}(z) \equiv -\nabla v_{\text{eff}}(z).$$

It is seen from Fig. 4 that force orientations are opposite at both sides of the film, so that the film in whole must be stressed. The existence of the force should lead to the increase of spacings between some lattice planes d, while spacings between other planes must become narrower.

The depth of the potential well, in which the electrons are located in metal film, decreases «in average» with increasing ε and, as a result, the electron work function $W = -\varepsilon_{\text{F}}(\kappa_{l,r}, \chi^{l,r} = 0)$ also decreases (see Fig. 5).

Film spectra $\{1|\text{Al}_L|1\}$ are presented in Fig. 5. For comparison, in the same figure, we also provide the results obtained within the electrons-in-a-box model with the well depth $U_0 = -(W_0 + \bar{\varepsilon}_{\text{F}}) < 0$.

It is seen from Fig. 5 that the dependence of the eigenstate energies on the film thickness, within the SJ model, is oscillating and decreasing. For subbands with large numbers $i = 10,11$, there are gaps due to the algorithm instability in the vicinity of the vacuum level. Within the rectangular-box

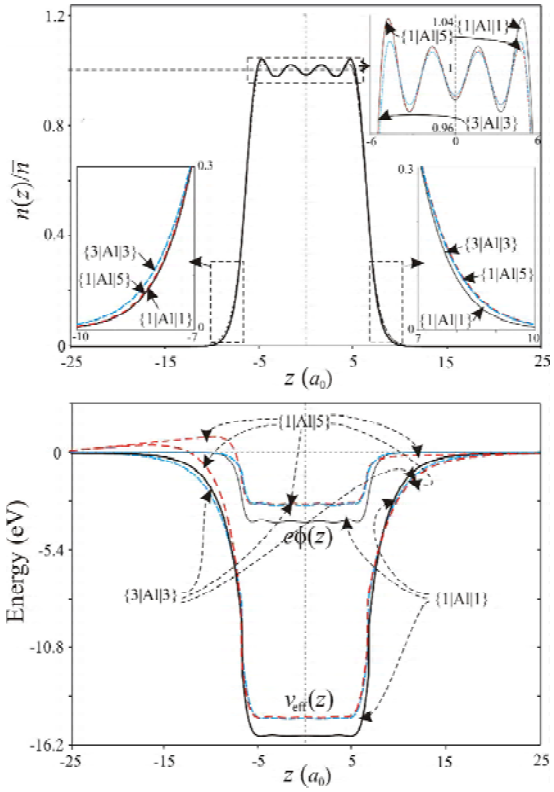

Fig. 4. The results of self-consistent calculations of the profiles of the one-electron effective potential $v_{eff}(z)$, and the electrostatic potential $\phi(z)$ for sandwiches: $\{1|\text{Al}|1\}$, $\{1|\text{Al}|5\}$ and $\{3|\text{Al}|3\}$ with $L = 2\bar{\lambda}_{\text{F}}$

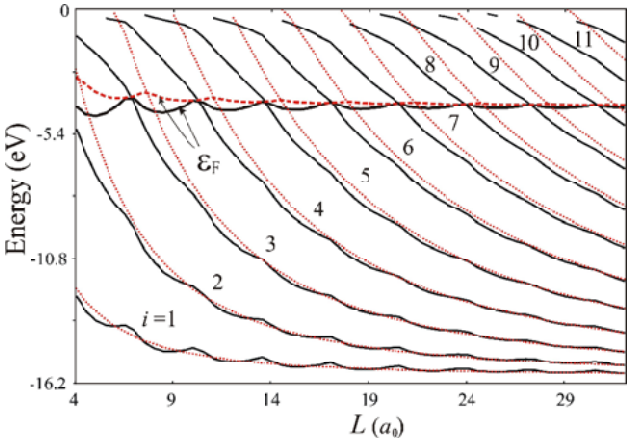

Fig. 5. Results of calculation for the energy spectrum (subbands) and Fermi energy $\varepsilon_{\text{F}}(L)$ of the film $\{1|\text{Al}|1\}$ by the self-consisting method (solid lines) and in rectangular-box model (dashed lines)

model, this dependence is only decreasing. Due to smoother edges of the self-consistent well, it contains more subbands compared to the model of a rectangular box. Difference in subbands numbers significantly affects calculated dielectric function and optical conductivity of the nanofilm [14].

Within the rectangular-box model, in contrast to the SJ model, $\varepsilon_{\text{F}}(L)$ is always located above one for 3D metal. Amplitudes of oscillations decrease as L increases. Within both models, maximum Fermi energies (minimum work functions (17)) correspond to the points, in which curves of eigenenergies intersect Fermi energies. Within the SJ model, in contrast to the rectangular-box model, minimum Fermi energies correspond to the points, in which Fermi energy is located between two nearest eigenenergies (magic film thicknesses similar to magic numbers in clusters).

Asymmetric sandwiches $\{\kappa_{\text{l}}|\text{Me}|\kappa_{\text{r}}\}$ and $\{1|\text{Me}|\kappa\}$, which contacts the air or vacuum, are of particular interest from the viewpoint of experimental investigation due to the perspective of their use in technological applications (see, for example, [5]).

Let us consider both electron density and potential profiles for the polycrystalline film $\{1|\text{Al}|5\}$. Presence of a dielectric at the right side of the film leads to the asymmetry of electron distribution (see the insets in Fig. 4), so that there appears a hump in both the electrostatic and effective potential at the left side above the vacuum level. This should result, for example, in the anisotropy of a field emission along the z-axis. It is worth mentioning that bottoms of wells for sandwiches $\{1|\text{Al}|5\}$ and $\{3|\text{Al}|3\}$ are essentially the same, some difference appears only in «tails» of potential profiles.

It is of interest to compare heights of humps at $L = 10;12;13,5$ and $20;\ 22;\ 23,5\ a_0$. These thicknesses correspond to the minimum, maximum, minimum of the dependence $W(L)$ for $\{1|\text{Al}|5\}$. It turns out that, with the increase of L, the hump height weakly oscillates and decays similarly to the work function, but maxima of the hump height corresponds to minima of the $W(L)$. For the values of L, as given above, these heights are 0,176; 0,148; 0,170 and 0,158; 0,139; 0,156 eV, respectively.

In order to analyze such a behavior of potential profiles, it is necessary to go beyond the isotropic model based on a defined (6) distribution of *homogeneous* positively charged background, i.e. one has to take into account not only the reaction of the electron subsystem, but also the reaction of the ion subsystem to the presence of a dielectric. Spacings between the lattice planes are determined by the balance of forces from the right and left sides for each plane. A simplest realization of this idea is to disregard variations of spacings between the lattice planes and to vary the profile of the ion jellium distribution (6). We found that such a procedure leads to a significant deformation of the well bottom, but does not result to considerable changes of both the spectrum and hump height.

Figs. 6 and 7 show results of our calculations of both the electron work function and surface energy for crystalline sandwiches using expression (23). Horizontal lines correspond to semiinfinite samples. In contrast to the surface energy, size dependences $W(L)$ have deep and pronounced minima. It is easier to analyze them using a simple model [12]. Amplitudes of largest work function «oscillations» are smaller than 0,5 eV. By considering dependencies for different metals, it is easy to see that all the differences are due to values of r_s. For the Al, which has the smallest r_s, work function oscillations are maximum, while the period is minimum. Positions of both maxima and minima depend weakly on ε of a dielectric and slightly shift towards smaller L with the increase κ.

In contrast to the work function, surface energy oscillations can be approximated by analytical dependences

$$E^{\mathrm{S}}\{\kappa\,|\,\mathrm{Me}_L\,|\,\kappa\} = E^{\mathrm{S}}\{\mathrm{Me}_\infty\,|\,\varepsilon\} + \Gamma\frac{\sin\left(2\bar{k}_{\mathrm{F}}L+\varphi\right)}{L},$$

with Γ and φ. Maxima of function $W(L)$, $\gamma(L)$, correspond to «magic» film thicknesses, which are defined by maximum occupation of a given subband.

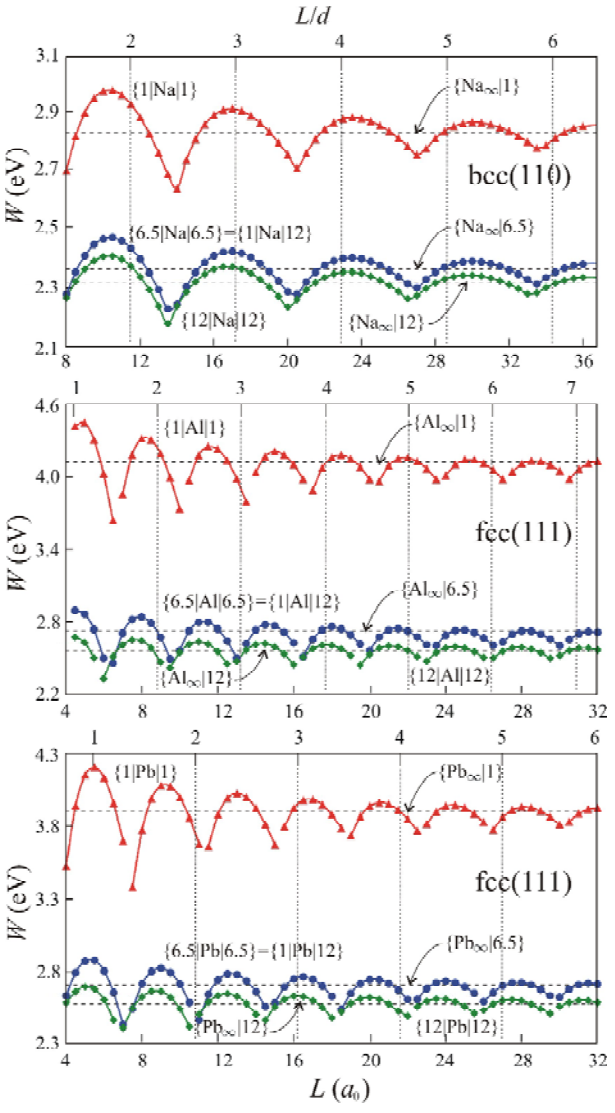

Fig. 6. Work function for crystalline sandwiches $\{\kappa_1\,|\,\mathrm{Me}\,|\,\kappa_\Gamma\}$ and semi-infinite metal covered by a dielectric $\{\mathrm{Me}_\infty\,|\,\kappa\}$ (Me ≡ Na, Al, Pb), $\chi = 0$

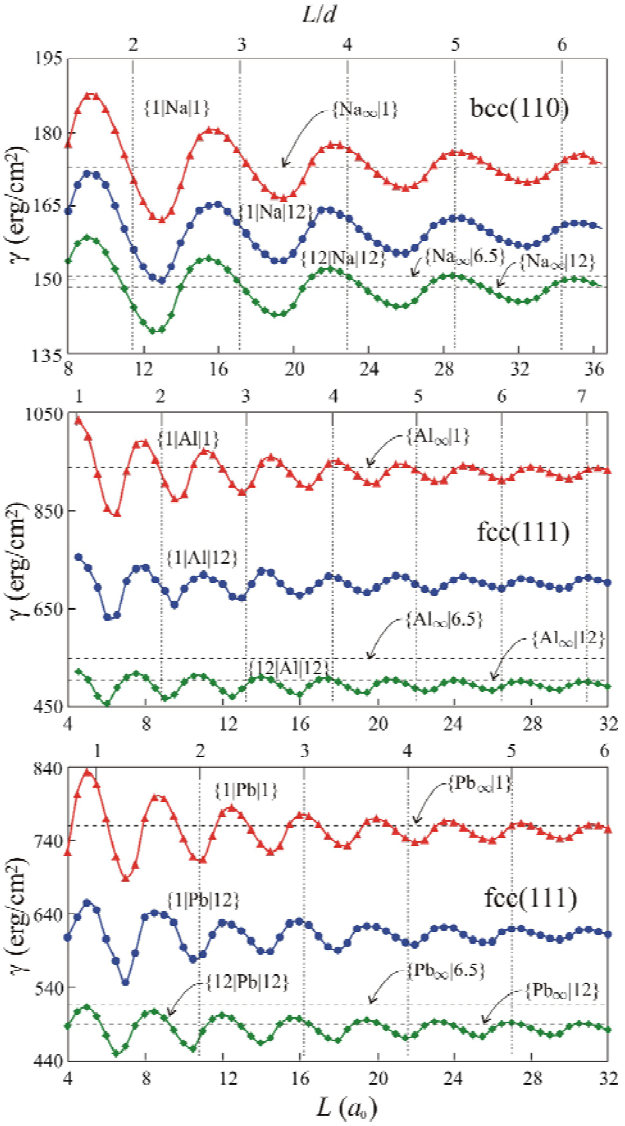

Fig. 7. Energy per unit of area for crystalline sandwiches $\{\varepsilon_1\,|\,\mathrm{Me}\,|\,\varepsilon_\Gamma\}$ and semi-infinite metal covered by a dielectric $\{\mathrm{Me}_\infty\,|\,\varepsilon\}$ (Me ≡ Na, Al, Pb), $\chi = 0$

The unexpectable result of self-consistent calculations is a coincidence of dependencies $W(L)$ for sandwiches $\{1|\mathrm{Me}|12\}$ and $\{6,5|\mathrm{Me}|6,5\}$. Computations for $\{1|\mathrm{Me}|5\}$ and $\{3|\mathrm{Me}|3\}$ give a similar result. This means that the electron work function for asymmetric sandwiches $\{\kappa_l|\mathrm{Me}|\kappa_r\}$ coincides with high accuracy with the work function for symmetric sandwiches $\{\langle\kappa\rangle|\mathrm{Me}|\langle\kappa\rangle\}$ with the averaged value $\langle\kappa\rangle = \frac{1}{2}(\kappa_l + \kappa_r)$.

Work function has both the bulk and surface contributions. Because bulk metal contributions $W(L)$ for sandwiches $\{1|\mathrm{Me}_L|12\}$ (like to vacuum/metal/Si) and $\{6,5|\mathrm{Me}_L|6,5\}$ are the same by definition, also the same are contributions of dipole surface barriers. We here imply the total contribution of both sides of a sandwich, since the work function is an «*isotropic*» characteristics [37]. A coincidence of work functions is most likely a geometric effect. This feature will be addressed elsewhere.

For surface energies, such a coincidence does not exist. It is not difficult to perform calculations according to formulas (21) and (22), if γ are known.

The results obtained by using the developed iteration procedure enable us to draw a conclusion about its efficiency. Moreover, one can follow the behavior of electron spatial profiles and potentials, as well as calculate a spectrum. The results in $\chi = 0$ and LDA approximation the provide reference data for simplified treatments.

(ii) Let us apply this approach ($\chi \neq 0$) to study an energetics of three samples with «ideal» interfaces: the film Al(111) on SiO_2 and on Al_2O_3, and the sandwich $SiO_2/Al/Al_2O_3$. For such a structure we use values from Table 1. $\chi^l = 0$ and $\kappa_l = 1$ and $\chi^{l,r}$ for vacuum/metal interface. For illustrative purposes, in Fig. 6 we present results of self-consistent calculations of potential profiles.

It turned out that all approaches give the same potential well depth as well as its profile near the bottom. Dependences $v_{xc}(z)$ at the left side of the film (in vacuum) are essentially the same according to approaches (i) and (ii), while for the right side of the plane they differ due to the presence of the conductivity band ($\chi \neq 0$) in the dielectric.

It should be noted that the use of nonlocal exchange-correlation potential in the iterative procedure leads to the essential disappearance of the potential hump in the effective potential (but not in the electrostatic one), which appears at the left side of the film, see Fig. 4.

In Table 2, we decided to present our data, which correspond to the scheme (ii) only. In all the approaches (i) and (ii), ε_F and surface energies differ from each other by less than 1 percent, while values of matching parameters can be rather different: for instance, $z_0^r = 5,95$ and $\lambda^r = 0,998$ for ML = 1 the film Al(111) on SiO_2 of the method (i). As a result, we conclude that our manipulations with the exchange-correlation potential did not lead to any noticeable changes of the Fermi level position, i.e. $\varepsilon_F(\langle\kappa\rangle, \chi^{l,r} = 0) \approx \varepsilon_F(\langle\kappa\rangle, \chi^{l,r} \neq 0)$.

We also performed computations for infinite-size systems ($L = \infty$): $W_d^r = 2,00$ and 1,48 eV for Al/SiO_2 and Al/Al_2O_3, respectively. However, in these calculations, it is not taken into account that the vacuum/metal interface exists at the left side of the samples. Therefore, the comparison with the data of Table 2 is not possible, since results do depend on the average dielectric constant of two media $\langle\kappa\rangle$, and not only on κ_r.

Our results point out that it is possible to control the Schottky barrier by tuning the metal film thickness (in the metal-insulator-semiconductor devices the thickness of gate insulating film is a tool to control the current in the channel [40]). For the evaluation of Fowler-Nordheim tunneling current [41], it is necessary to know a spatial profile of the effective potential, which should be added to the external electrostatic potential $\varphi_{ext}(z)$, starting from points at $z = Z^{l,r}$.

Let us compare our results with experimental data. The calculated work function for the interface Al(111)/vacuum is 4,12 eV; the experimental one $\in (3.11,4.26)$ eV [42]; and 4,28 eV for polycrystalline Al [43]. Recommended $\chi = 3,03$ and 3,3 eV in [44], corresponding for SiO_2 and Al_2O_3, differ from data in Table 1. The measured Schottky barrier height [44] for Au/Al_2O_3 equals $3,5 \pm 0,1$ eV. Note that experimental values of work function for Au and Al in Ref. [42] are close to each other, while they differ by almost 1 eV, according to Ref. [43].

On the other hand, the measured Schottky barrier heights in Ref. [45] for Al, Ag and Cu, placed on thick (by thickness 35 nm) film of Al_2O_3, equal 1,66; 1,72 and 1,80 eV, respectively. It is in accordance with 1,5 eV for Al/Al_2O_3 [39] and the results from Table 2. As we see, experimental data are rather diverse.

An important question is under which conditions our approach becomes questionable. When $|\varepsilon_F| \leq \chi^{l,r}$, our model does not work. In accordance with Fig. 5 and Table 1, values $W_d \in (0,4;0,75)$ eV for Al/Si, Pb/Si [39] and $W_d \in (0,49;0,6)$ eV for thick films of Ti ($L \in (50,90)$ nm) on the Si-substrate [46] should correspond to the regime $|\varepsilon_F| \leq \chi^{l,r}$. The efficient approach in this case is the local density formalism pseudopotential method [47, 48, 49, 50]. In our approach, it is also not possible to take into account the role of virtual gap states and defects in metal-dielectric contacts [51]. Nevertheless, we expect that our method provides a correct estimate for the size dependence of

Table 1. The examles of simplest coating and substrates [38, 39]

Material	He	Ne	Ar	Kr	Xe	SiO_2	Al_2O_3	Si
κ	1,10	1,20	1,50	1,65	1,90	4	9	13
χ, eV	–1,0	0,10	0,20	0,45	0,68	1,1	1,35	4,05

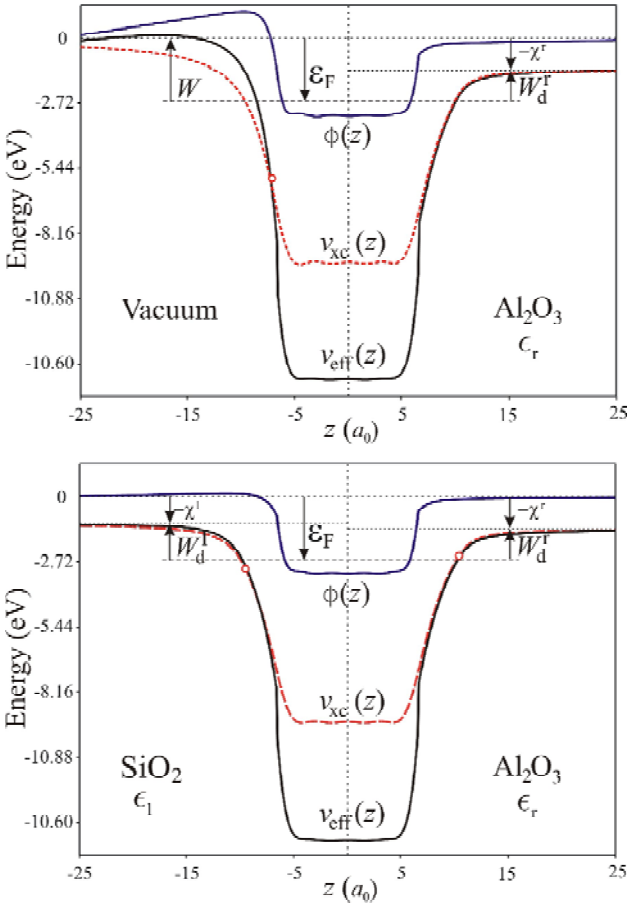

Fig. 8. The self-consistent profiles of electrostatic, exchange-correlation and effective potentials for the sandwiches vacuum/Al(111)/Al_2O_3 and SiO_2/Al(111)/Al_2O_3. The thickness of film L=3ML. 1ML=4,4a_0

characteristics of films in contact with dielectrics, for which κ and χ are not large.

The effect of temperature was studied earlier in Ref. [26] when determining ionization potential of metallic cluster. It turns out that the effect is not significant at room temperatures, as it can be expected. For the film-dielectric contact, of importance is the ratio of $-\chi^r$ and the Fermi energy. If these quantities are comparable, the result should be sensitive to the system temperature.

4. SUMMARY AND CONCLUSIONS

We proposed a method for the self-consistent calculations of spectra, electron work function, and surface energy of metal films placed into passive dielectrics. As typical examples, we considered Na, Al, and Pb films.

The effective force acting on the film from the outside is due to the inhomogeneous electron distribution. This force should lead to film stressing in a transverse direction. The effect of the stressing generally becomes more significant with the increase of the film thickness.

In contrast to the surface energy, size dependencies of work function have deep and strongly pronounced minima. The smaller r_s the more difficult the problem of numerical analysis of size dependencies in the vicinities of these minima.

With the increase of film thickness up to few $\overline{\lambda}_F$, size variations of both the work function and surface energy occur near their average values (for symmetric sandwiches, these values correspond to 3D metals and do not contain significant monotonous size contributions). Dielectric environment generally leads to the decrease of electron work function and surface energy.

Table 2. Calculated values for film Al(111) of thickness L (in monolayers) on SiO_2 (upper numbers), Al_2O_3 (middle numbers), and the sandwiche SiO_2/Al_2O_3 (lower numbers)

L, ML	z_0^l, a_0	z_0^r, a_0	λ^l, a_0	λ^r, a_0	W_d^l, eV	W_d^r, eV	γ, erg/cm^2
1	1,05	3,35	0,977	0,706	3,43	2,33	821
	1,00	4,25	0,962	0,518	3,01	1,66	760
	3,30	4,15	0,707	0,519	1,79	1,54	607
2	0,95	2,85	0,946	0,643	3,26	2,16	755
	0,95	3,60	0,945	0,474	2,84	1,49	704
	2,85	3,60	0,640	0,479	1,62	1,37	548
3	0,85	2,60	0,921	0,606	2,94	1,84	734
	0,85	3,50	0,919	0,476	2,63	1,28	696
	2,95	3,80	0,672	0,512	1,56	1,31	562
4	0,90	3,05	0,933	0,683	3,23	2,13	779
	0,95	4,05	0,948	0,531	2,86	1,51	735
	3,10	4,05	0,688	0,535	1,69	1,44	578
5	0,90	2,95	0,932	0,661	3,23	2,13	764
	0,95	3,85	0,948	0,507	2,84	1,49	716
	3,00	3,85	0,671	0,512	1,65	1,40	556
6	0,90	2,85	0,934	0,651	3,13	2,03	751
	0,90	3,65	0,933	0,489	2,73	1,38	705
	2,85	3,65	0,645	0,491	1,54	1,29	550
7	0,90	2,95	0,934	0,669	3,17	2,07	770
	0,90	3,90	0,933	0,520	2,80	1,45	726
	3,05	3,95	0,684	0,527	1,65	1,40	569

We also considered asymmetric metal-dielectric sandwiches characterized by different dielectrics at both sides of the film. One of the examples of such systems is a film on the dielectric substrate. We found that the presence of a dielectric from one side of the film leads to such a «deformation» of electron distribution that there appears a «hump» above the vacuum level both in the electrostatic and effective potentials. The asymmetry of potential profile should lead to an anisotropy of the field emission. In addition to size dependencies, the shift of the work function is generally determined by the average dielectric constants of environments.

We introduced the position of a conductivity band in the dielectric as a parameter in the self-consistency procedure and performed calculations for the aluminum film on SiO_2 and Al_2O_3, using a nonlocal exchange-correlation potential. As a result, profiles of electron concentration, effective potential, and energy spectrum were calculated.

Finally, let us formulate some methodological conclusions:

(i) An introduction of nonlocal potential, as well as the position of conductivity band in dielectric material does not lead to significant changes of Fermi level of a metal film contacting with a dielectric.

(ii) Accounting for the conductivity band in a dielectric and self-consistency condition for the potential well shape, one changes the spectrum (subbands number), as well as the density of states. Therefore, matrix elements of optical transitions are also changed, which leads to the modification of optical absorption coefficient [14]. Equilibrium profile of electrons and electrostatic potential is needed to calculate the field emission of electrons as well as annihilation characteristics of positrons in nanostructures.

We thank W. V. Pogosov for reading the manuscript.

APPENIX: SELF-CONSISTENCY PROCEDURE

The initial approximation $n(z)$ is chosen for solving the Kohn-Sham equations in the form of a one-parametric trial function $n^{(0)}(z) = \bar{n} f(z)$, where

$$f(z) = \begin{cases} -\frac{1}{2} e^{(z-L/2)/\lambda} + \frac{1}{2} e^{(z+L/2)/\lambda}, & z < -L/2, \\ 1 - \frac{1}{2} e^{(z-L/2)/\lambda} - \frac{1}{2} e^{-(z+L/2)/\lambda}, & |z| < L/2, \\ -\frac{1}{2} e^{-(z+L/2)/\lambda} + \frac{1}{2} e^{-(z-L/2)/\lambda}, & z > L/2. \end{cases}$$

λ is the variational parameter, which is found through the minimization of surface energy. Solution by a direct variational method is an independent problem, which is not addressed in this paper (for simple metals λ is closed to $1a_0$). As a result of integration of equation (9), within the initial approximation, we obtain $\phi^{(0)}(z) = -4\pi\bar{n}\lambda^2 f(z)$.

Each wave function $\psi(z)$ is constructed as

$$\psi(z) = \begin{cases} \psi_{\text{left}}(z), & z < z_0, \\ \psi_{\text{right}}(z), & z > z_0, \end{cases}$$

under the condition of continuity of functions $\psi_{\text{left}}(z_0) = \psi_{\text{right}}(z_0)$, as well as of their derivatives $\psi'_{\text{left}}(z_0) = \psi'_{\text{right}}(z_0)$. z_0 is an arbitrary point in the interval $z \in [-L/2; +L/2]$, while $\psi_{\text{left}}(z)$ and $\psi_{\text{right}}(z)$ are functions, which are found by a numerical solution of Eq. (7) by the Numerov's method from $z = z_-$ to $z = z_0$ and from $z = z_+$ to $z = z_0$, respectively. It is sufficient to take values $z_{\mp} = \mp(L + 20)a_0$. In these points, the potential profile $v_{\text{eff}}(z)$ is cut off. The boundary conditions (7) here are determined by the behavior of the wave function ψ under the barrier from the left ($e^{z\sqrt{|\varepsilon_i|}}$) and right ($e^{-z\sqrt{|\varepsilon_i|}}$) sides from the slab ($|z| \geq |z_{\mp}|$) respectively. Boundary conditions provide wave function, as well as its derivative at $z = z_{\mp}$. This peculiarity of our computations is due to the fact that errors of the numerical method for the wave function $\psi_{\text{right}}(z)$ and $\psi_{\text{left}}(z)$ near the right and left boundaries of the interval grow, since the round-off errors also increase and lead to the instability of the algorithm under the motion towards the exponential damping.

In order to solve the system of equations (7), (9) and (15) self-consistently, with relatively small number of iteration steps, the Poisson equation (9) should be modified, in particular, by introducing a perturbation [52].

Equation (9) is solved by the Lagrange method in the form

$$\phi^{(j)\prime\prime} - q^2\phi^{(j-1)} = \phi - \frac{4\pi}{\kappa(z)}\left[n^{(j)} - \rho\right] - q^2\phi^{(j-1)} \qquad (27)$$

with the boundary conditions

$$\begin{aligned} &\phi^{(j)}_{\text{out}}(z) = \phi^{(j)}_{in}(z), \quad \kappa_1\phi^{(j)\prime}_{out}(z) = \phi^{(j)\prime}_{in}(z); \quad z = -L/2, \\ &\phi^{(j)}_{in}(z) = \phi^{(j)}_{out}(z), \quad \phi^{(j)\prime}_{in}(z) = \kappa_r\phi^{(j)\prime}_{out}(z); \quad z = L/2, \\ &\phi^{(j)}_{out}(z) = 0, \qquad \phi^{(j)\prime}_{out}(z) = 0; \qquad z = \mp\infty. \end{aligned} \qquad (28)$$

The term $q^2\phi$ was introduced as a small perturbation; $\phi_{\text{out}}(z)$ and $\phi_{\text{in}}(z)$ are potentials outside and inside the film, respectively. In equation (27), at each step of the iteration $j = 1,2,3,\ldots$, electrostatic potential profile depends not only on the electronic concentration profile, but also on its own profile at the previous iteration. It is convenient to take q equal to electron wave number at the Fermi sphere $\bar{k}_{\text{F}} = (3\pi^2\bar{n})^{1/3}$ of homogeneous electron liquid.

In view of the multimolecular thicknesses of dielectric coatings on the metal film surfaces and rapid fall of the electron distribution outside of a film (approximately at a distance of 10–15 a_0), we formally neglected the effect of a thickness of the coatings, whose minimum thicknesses must be much greater than that of a monatomic (molecular) layer of a dielectric. The solution of equation (27) for $\Lambda \to \infty$ has the simple form

$$\phi^{(j)}(z)=\begin{cases}\left(\int\limits_{-\infty}^{z}\frac{e^{-qz'}}{2q}f_1dz'+A_1\right)e^{qz}+\left(-\int\limits_{-\infty}^{z}\frac{e^{qz'}}{2q}f_1dz'+B_1\right)e^{-qz}, z<-L/2,\\ \left(\int\limits_{-L/2}^{z}\frac{e^{-qz'}}{2q}f_2dz'+A_2\right)e^{qz}+\left(-\int\limits_{-L/2}^{z}\frac{e^{qz'}}{2q}f_2dz'+B_2\right)e^{-qz}, |z|\le L/2,\\ \left(-\int\limits_{z}^{\infty}\frac{e^{-qz'}}{2q}f_3dz'+A_3\right)e^{qz}+\left(\int\limits_{z}^{\infty}\frac{e^{qz'}}{2q}f_3dz'+B_3\right)e^{-qz}, z>L/2,\end{cases} \quad (29)$$

where $f_m(z')=-4\pi[n(z')-\rho(z')]D_m-q^2\phi^{(j-1)}(z')$ and $D_m=\kappa_l^{-1},1,\kappa_r^{-1}$ for $m=1,2,3$, respectively. The choice of values $B_1=0$ and $A_3=0$ immediately follows from the condition of finiteness of potentials far away from the film.

Values of other coefficients A and B are found from the solution of the system of equations (28):

$$A_1=\frac{2A_2}{1+\kappa_l}+\frac{1-\kappa_l}{1+\kappa_l}\int\limits_{-\infty}^{-L/2}\frac{e^{q(z'+L)}}{2q}f_1dz'-\int\limits_{-\infty}^{-L/2}\frac{e^{-qz'}}{2q}f_1dz',$$

$$B_3=\frac{2B_2}{1+\kappa_r}-\frac{1}{1+\kappa_r}\int\limits_{-L/2}^{L/2}\frac{e^{qz'}}{q}f_2dz'+$$

$$+\frac{1-\kappa_r}{1+\kappa_r}\int\limits_{L/2}^{\infty}\frac{e^{-q(z'-L)}}{2q}f_3dz'-\int\limits_{L/2}^{\infty}\frac{e^{qz'}}{2q}f_3dz'.$$

Let's introduce notation

$$J_{(\pm)}=Y_0\left[Y_1 2\kappa_l(1\mp\kappa_r)\int\limits_{-\infty}^{-L/2}dz'e^{qz'}f_1+Y_2(1\pm\kappa_l)(1+\kappa_r)\times\right.$$

$$\times\int\limits_{-L/2}^{L/2}dz'e^{-qz'}f_2+Y_3(1\pm\kappa_l)(1-\kappa_r)\times$$

$$\left.\times\int\limits_{-L/2}^{L/2}dz'e^{qz'}f_2+Y_4 2\kappa_r(1\pm\kappa_l)\int\limits_{L/2}^{\infty}dz'e^{-qz'}f_3\right], \quad (30)$$

where

$$Y_0=\{2q[(1-\kappa_l)(1-\kappa_r)e^{-qL}-(1+\kappa_l)(1+\kappa_r)e^{qL}]\}^{-1}.$$

Then $A_2=J_{(+)}$ for $Y_{1,3}=1, Y_{2,4}=e^{qL}$ and $B_2=J_{(-)}$ for $Y_{2,4}=1, Y_1=e^{qL}=Y_3^{-1}$.

In the case of the symmetric sandwich $\kappa_l=\kappa_r$ the accurateness of calculations is verified by examination the stationarity conditions $n'(z)=0$ and $\varphi_{in}^{(i)\prime}(z)=0$ in the center of the slab ($z=0$).

SPISOK LITERATURY

1. *Otero, R.* Observation of preferred heights in Pb nanoislands: A quantum size effect / R. Otero, A. L. Vazquez de Parga and R. Miranda // Phys. Rev. B. – 2002. – V. 66, № 11. – P. 115401.
2. *Pagge, J. J.* Atomic-layer-resolved quantum oscillations in the work function: Theory and experiment for Ag/Fe(100) / J. J. Paggel, C. M. Wei, M. Y. Chou // Phys. Rev. B. – 2002. – V. 66, № 23. – P. 115401.
3. *Buturovich, D. V.* Friedel oscillations in ytterbium films deposited on the Si(111) 7 x 7 surface / D. V. Buturovich, M. V. Kuz'min, M. V. Loginov // Physics of the Solid State. – 2006. – V. 48, № 11. – P. 2205–2208.
4. *Liu, Y.* Quantized electronic structure and growth of Pb films on highly oriented pyrolytic graphite / Y. Liu, J. J. Paggel, M. H. Upton, T. Miller and T.-C. Chiang // Phys. Rev. B. – 2008. – V. 78, № 23. – P. 235437.
5. *Chiang, T.-C.* Quantum physics of thin metal films / Chiang T.-C. // Bulletin of AAPPS. – 2008. – V.81, №2. – P. 2–10.
6. Quantum oscillations in surface properties / [Vazquez de Parga A. L., Hinarejos J. J., Calleja F. and other] // Surface Science. – 2009. – V. 603. – P. 1389–1396.
7. *Vinogradov N.A.,* Size effects in ultrathin Mg/W(110) films: Quantum electronic states / N. A. Vinogradov, D. E. Marchenko, A. M. Shikin // Phys. Sol. State. – 2009. – V. 51. – P. 179.
8. Consonant diminution of lattice and electronic coupling between a film and a substrate: Pb on Ge(100) / Chen P.-W., Lu Y.-H., Chang T.-R., Wang C.-B. // Phys. Rev. B. – 2011. – V.84, № 20 – P. 205401.
9. Self-consistent study of electron confinement to metallic thin films on solid surfaces / [Ogando E., Zabala N., Chulkov E. V., Puska M. J.] // Phys. Rev. B. – 2005. – V.71, № 20. – P. 205401.
10. *Rogers III J. P.,* Quantum size effects in the fermi energy and electronic density of states in a finite square well thin film model / Rogers III J. P., Cutler P. H., Feuchtwang T. E. // Surface Science. – 1987. – V. 181. – P. 436–456.
11. *Moskalets, M. V.* The quantum size electrostatic potential in two-dimensional point ballistic contacts / M. V. Moskalets // JETP Lett. – 1995. – V. 62. – P. 719–722.
12. *Pogosov, V. V.* Energetics of metal slabs and clusters: The rectangular-box model / V. V. Pogosov, V. P. Kurbatsky, E. V. Vasyutin // Phys. Rev. B. – 2005. – V. 71, № 19. – P. 195410.
13. *Han, Y.* Quantum size effects in metal nanofilms: Comparison of an electron-gas model and density functional theory calculations / Y. Han, D.-J. Liu // Phys. Rev. B. – 2009. – V. 80, № 7. – P. 155404.
14. *Kurbatsky, V. P.* Optical conductivity of metal nanofilms and nanowires: The rectangular-box model / V. P. Kurbatsky, V. V. Pogosov // Phys. Rev. B. – 2010. – V. 81, № 15. – P. 155414.
15. *Dymnikov, V. D.* Fermi energy of electrons in a thin metallic plate / V. D. Dymnikov // Phys. Sol. State. – 2011. – V. 53, № 5 – P. 901–907.

16. *Schulte, F. K.* A theory of thin metal films: electron density, potentials and work function / F. K. Schulte // Surface Science. – 1976. – V. 55. – P. 427–444.
17. *Zabala, N.* Electronic structure of cylindrical simple-metal nanowires in the stabilized jellium model / N. Zabala, M. J. Puska, R. M. Nieminen // Phys. Rev. B. – 1999. – V. 59, № 19. –P. 12652–12660.
18. *Sarria, I.* Slabs of stabilized jellium: Quantum-size and self-compression effects / I. Sarria, C. Henriques, C. Fiolhais // Phys. Rev. B. – 2000. – V. 62, № 3. – P. 1699–1705.
19. *Smogunov, A. N.* Electronic structure and polarizability of quantum metallic wires / A. N. Smogunov, L. I. Kurkina, O. V. Farberovich // Phys. Solid State. – 2000. – V. 42. – P. 1898–1907.
20. *Horowitz, C. M.* Position-dependent exact-exchange energy for slabs and semi-infinite jellium / C. M. Horowitz, L. A. Constantin, C. R. Proetto // Phys. Rev. B. – 2009. – V.80, № 23. – P. 235101.
21. *Feibelman, P. J.* Quantum-size effects in work functions of free-standing and adsorbed thin metal films / *P. J. Feibelman* // Phys. Rev. B. – 1984. – V. 29, № 3. – P. 6463–6467.
22. *Boettger, J. C.* Persistent quantum-size effect in aluminum films up to twelve atoms thick / J. C. Boettger // Phys. Rev. B. – 1996. – V. 53, №19. – P. 13133–13137.
23. *Zhang, Z.* Electronic Growth of Metallic Overlayers on Semiconductor Substrates / Z. Zhang, Q. Niu, C.-K. Shih // Physical Review Letters. – 1998. – V. 80, № 24. – P. 5381–5384.
24. *Kiejna, A.* Quantum-size effect in thin Al(110) slabs / A. Kiejna, J. Peisert, P. Scharoch // Surface Science. – 1999. – V. 432, № 1–2. – P. 54–60.
25. *Pogosov, V. V.* Sum-rules and energy characteristics of small metal particle / V. V. Pogosov // Solid State Communications. – 1990. – V. 75, № 5. – P. 469–472.
26. *Kiejna, A.* On the temperature dependence of the ionization potential of self-compressed solid- and liquid-metallic clusters / A. Kiejna, V. V. Pogosov // Journal of Physics: Condensed Matter. – 1996. – V. 8. – № 23. – P. 4245–4257.
27. *Hirabayashi, K.* Dielectric theory of the barrier height at metal-semiconductor and metal-insulator interfaces / K. Hirabayashi // Phys. Rev. B. – 1971. – V. 3, № 12. – P. 4023–4025.
28. *Puska, M. J.* Electronic polarisability of small metal spheres / M. J. Puska, R. M. Nieminen, M. Manninen // Phys. Rev. – 1985. – B 31. – P. 3486.
29. *Rubio, A.* Dielectric screening effects on the photoabsorption cross section of embedded metallic clusters / A. Rubio, L. Serra // Phys. Rev. B. – 1993. – V.48, № 24. – P. 18222–18229.
30. *Perdew, J. P.* Stabilized jellium: Structureless pseudopotential model for the cohesive and surface properties of metals / Perdew J. P., Tran H. Q., Smith E. D. // Phys. Rev. Lett. – 1990. – V.42, № 18. – P. 11627–11636.
31. *Perdew, J. P.* Self-interaction correction to density-functional approximations for many-electron systems / J. P. Perdew, A. Zunger // Phys. Rev. B. – 1981. – V. 23, № 10. – P. 5048–5079.
32. *Babich, A. V.* Effect of dielectric coating on the electron work function and the surface stress of a metal / *A. V. Babich, V. V. Pogosov* // Surface Science. – 2009. – V. 603, № 16. – P. 2393–2397.
33. *Serena, P.A.* Self-consistent image potential in a metal surface / *P. A. Serena, J. M. Soler, N. Garcia* // Phys. Rev. B. – 1986. – V. 34. – P. 6767–6769.
34. *Constantin, L. A.* Adiabatic-connection-fluctuation-dissipation approach to long-range behavior of exchange-correlation energy at metal surfaces: A numerical study for jellium slabs / L. A. Constantin, J. M. Pitarke // Phys. Rev. B. – 2011. – V. 83. – № 7. – P. 075116.
35. *Lang, N. D.* Theory of Metal Surfaces: Charge Density and Surface Energy / N. D. Lang, W. Kohn // Phys. Rev. B. – 1970. – V.1. – P. 4555.
36. *Pogosov V. V.*, On some tenzoemission effects of the small metal particles / V. V. Pogosov // Chem. Phys. Lett. – 1993. – V. 193. – P. 129.
37. *Pogosov V. V.,* Density-Functional Theory of Elastically Deformed Finite Metallic System: Work Function and Surface Stress / V. V. Pogosov, V. P. Kurbatsky // Journal of Experimental and Theoretical Physics. – 2001. – V. 92, № 2 – P. 304–311.
38. *Stampfli P.*, Theory for the electron affinity of clusters of rare gas atoms and polar molecules / *P. Stampfli* // Phys.Rep. – 1995. – V. 255 – P. 1–77.
39. *Rhoderick, E. H.* Metal-semiconductor contacts / E. H. Rhoderick. – Clarendon Press, Oxford, 1978. – 252 p.
40. *Lin, L.* Identifying a suitable passivation route for Ge interfaces / L. Lin, H. Li, J. Robertson // Appl. Phys. Lett. – 2012. – V. 101 – P. 172907.
41. *Fowler, R. H.* Electron Emission in Intense Electric Fields / R. H. Fowler, L. Nordheim // Proc. Roy. Soc. –1928. – A 119. – 173 p.
42. *Фоменко, В. С.* Эмиссионные свойства материалов / В. С. Фоменко. – К. : Наукова думка, 1981. – 339 с.
43. *Michaelson, H. B.* The work function of the elements and its periodicity / H. B. Michaelson // J. Appl. Phys. – 1977. – V. 48. – P. 4729.
44. *Brewer, J. C.* Determination of energy barrier profiles for high-k dielectric materials utilizing bias-dependent internal photoemission / J. C. Brewer, R. J. Walters, L. D. Bell // Appl. Phys. Lett. – 2004. – V. 85. – P. 4133.
45. *Singh, K.* Current-Voltage Characteristics and Photoresponse of Metal Metal Devices / K. Singh and S.N.A. Hammond // Tur. J. of Phys. – 1998. – V. 22 – № 4 – P. 315.
46. *Jang, Moongyu* Analysis of Schottky Barrier Height in Small Contacts Using a Thermionic-Field Emission Model / Moongyu Jang, Junghwan Lee // ETRI Journal. – 2002. – V. 24. – № 6. – P. 455–461.
47. *Louie, S. G.* Electronic structure of a metal-semiconductor interface / S. G. Louie, M .L. Cohen // Phys. Rev. B. – 1976. – P. 2461.
48. *Bordier, G.* Electronic structure of a metal-insulator interface: Towards a theory of nonreactive adhesion / G. Bordier, C. Noguera // Phys. Rev. B. – 1991. – V. 44, № 12. – P. 6361–6371.
49. *Zavodinsky, V. G.* Schottky barrier formation in the Au/Si nanoscale system : A local density approximation study / V. G. Zavodinsky, I. A. Kuyanov // J. Appl. Phys. – 1997. – V. 81, № 6. – P. 2715–2759.
50. *Peacock, P. W.* Band offsets and Schottky barrier heights of high dielectric constant oxides / P. W. Peacock, J. Robertson // J. Appl. Phys. – 2002. – V. 92 – P. 4712–4722.
51. *Mцnch, W.* Role of virtual gap states and defects in metal-semiconductor contacts / W. Mцnch // Phys. Rev. Lett. – 1987. – V. 58, № 12. – P. 1260–1263.
52. *Arponen, J.* Charge density and positron annihilation at lattice defects in aluminium / J. Arponen, P. Hautojarvi, R. Nieminen // Journal of Physics F: Metal Physics. – 1973. – V. 3. – P. 2092.

Стаття надійшла до редакції 14.01.2013.
Після доробки 29.01.2013.

Бабич А. В.[1], Погосов В. В.[2], Вакула П. В.[3]
[1]Канд. физ.-мат. наук, доцент, Запорожский национальный технический университет, Украина
[2]Д-р физ.-мат. наук, профессор, Запорожский национальный технический университет, Украина
[3]Асистент, Запорожский национальный технический университет, Украина

САМОСОГЛАСОВАННЫЕ РАСЧЕТЫ РАБОТЫ ВЫХОДА, ВЫСОТЫ БАРЬЕРА ШОТТКИ И ПОВЕРХНОСТНОЙ ЭНЕРГИИ МАТАЛЛИЧЕСКИХ НАНОПЛЕНОК В ДИЭЛЕКТРИЧЕСКОМ ОКРУЖЕНИИ

Предложен метод самосогласованных вычислений характеристик металлической пленки в диэлектриках. В рамках модифицированного метода Кона-Шэма и модели стабильного желе рассчитан наиболее интересный (асимметричный) случай металл-диэлектрических сандвичей: разных диэлектриков по обе стороны пленки. На примере Al и Na впервые вычислены спектр, работа выхода электронов и поверхностная энергия поликристаллических пленок, помещенных в пассивные изоляторы. Диэлектрическое окружение в целом приводит к отрицательному изменению работы выхода электронов и поверхностной энергии. Помимо размерных изменений сдвиг работы выхода определяется среднеарифметическим значением диэлектрических констант окружающих сред. С учетом сил изображения и зоны проводимости диэлектрика выполнены самосогласованные вычисления профилей потенциалов, работ выхода и барьеров Шоттки для нанопленок алюминия с идеальными интерфейсами вакуум/ Al(111)/SiO_2, вакуум/ Al(111)/Al_2O_3 и сандвича SiO_2/Al(111)/Al_2O_3.

Ключевые слова: металлические нанопленки, диэлектрик, работа выхода, поверхностная энергия, высота барьера Шоттки.

Бабіч А. В.[1], Погосов В. В.[2], Вакула П. В.[3]
[1]Канд. фіз.-мат. наук, доцент, Запорізький національний технічний університет, Україна
[2]Д-р фіз.-мат. наук, професор, Запорізький національний технічний університет, Україна
[3]Асистент, Запорізький національний технічний університет, Україна

САМОУЗГОДЖЕНІ РОЗРАХУНКИ РОБОТИ ВИХОДУ, ВИСОТИ БАР'ЄРУ ШОТТКІ І ПОВЕРХНЕВОЇ ЕНЕРГІЇ МЕТАЛЕВИХ НАНОПЛІВОК В ДІЕЛЕКТРИЧНОМУ ОТОЧЕННІ

Запропоновано метод самоузгоджених обчислень характеристик металевої плівки в діелектриках. В рамках модифікованого методу Кона-Шема і моделі стабільного желе розрахований найбільш цікавий (асиметричний) випадок метал-діелектричних сендвічів: різних діелектриків по обидві сторони плівки. На прикладі Al і Na вперше розраховані спектр, робота виходу електронів і поверхнева енергія полікристалічних плівок, поміщених в пасивні ізолятори. Діелектричне оточення в цілому призводить до негативної зміни роботи виходу електронів і поверхневої енергії. Крім розмірних змін зсув роботи виходу визначається середньоарифметичним значенням діелектричних констант навколишніх середовищ. З урахуванням сил зображення та зони провідності діелектрика виконані самоузгоджені обчислення профілів потенціалів, робіт виходу і бар'єрів Шотткі для наноплівок алюмінію з ідеальними інтерфейсами вакуум Al(111)/SiO_2, вакуум/ Al(111)/AlO і сандвіча SiO/Al(111)/AlO.

Ключові слова: металеві наноплівки, діелектрик, робота виходу, поверхнева енергія, висота бар'єру Шотткі.

REFERENCES

1. Otero R., Vazquez de Parga A. L., Miranda R. Observation of preferred heights in Pb nanoislands: A quantum size effect, Phys. Rev. B., 2002, V. 66, No. 11, 115401 p.
2. Paggel J. J., Wei C. M., Chou M. Y, Atomic-layer-resolved quantum oscillations in the work function: Theory and experiment for Ag/Fe(100), *Phys. Rev. B.*, 2002, V.66, No. 23, 115401 p.
3. Buturovich D. V., Kuz'min M. V., Loginov M. V., Friedel oscillations in ytterbium films deposited on the Si(111) 7 x 7 surface, *Physics of the Solid State*, 2006, V. 48, No. 11, pp. 2205–2208.
4. Liu Y., Paggel J. J., Upton M. H., Miller T., Chiang T.-C., Quantized electronic structure and growth of Pb films on highly oriented pyrolytic graphite, *Phys. Rev. B.,* 2008, V. 78, No. 23, 235437 p.
5. Chiang T.-C., Quantum physics of thin metal films, *Bulletin of AAPPS*, 2008, V. 81, № 2, pp. 2–10.
6. Vazquez de Parga A. L., Hinarejos J. J., Calleja F., Camarero J., Otero R., Miranda R., Quantum oscillations in surface properties, *Surface Science*, 2009, V. 603, pp. 1389–1396.
7. Vinogradov N. A., Marchenko D. E., Shikin A. M., Size effects in ultrathin Mg/W(110) films: Quantum electronic states, Phys. Sol. State, 2009, V. 51, 179 p.
8. Chen P.-W., Lu Y.-H., Chang T.-R., Wang C.-B., Consonant diminution of lattice and electronic coupling between a film and a substrate: Pb on Ge(100), *Phys. Rev. B*, 2011, V. 84, No. 20, 205401 p.
9. Ogando E., Zabala N., Chulkov E. V., Puska M. J., Self-consistent study of electron confinement to metallic thin films on solid surfaces, *Phys. Rev. B.*, 2005, V. 71, No. 20, 205401 p.
10. Rogers III J. P., Cutler P. H., Feuchtwang T. E., Quantum size effects in the fermi energy and electronic density of states in a finite square well thin film model, *Surface Science*, 1987, V. 181, pp. 436–456.
11. Moskalets M. V., The quantum size electrostatic potential in two-dimensional point ballistic contacts, *JETP Lett.*, 1995, V. 62, pp. 719–722.
12. Pogosov V. V., Kurbatsky V. P., Vasyutin E. V., Energetics of metal slabs and clusters: The rectangular-box model, *Phys. Rev. B.*, 2005, V. 71, No. 19, 195410 p.
13. Han Y., Liu D.-J. Quantum size effects in metal nanofilms: Comparison of an electron-gas model and density functional theory calculations, *Phys. Rev. B.*, 2009, V. 80, No. 7, 155404 p.
14. Kurbatsky V. P., Pogosov V. V. Optical conductivity of metal nanofilms and nanowires: The rectangular-box model, *Phys. Rev. B.,* 2010, V. 81, No. 15, 155414 p.
15. Dymnikov V. D., Fermi energy of electrons in a thin metallic plate, *Phys. Sol. State*, 2011, V. 53, No. 5, pp. 901–907.
16. Schulte F. K., A theory of thin metal films: electron density, potentials and work function, *Surface Science*, 1976, V. 55, pp. 427–444.
17. Zabala N., Puska M. J., Nieminen R. M. Electronic structure of cylindrical simple-metal nanowires in the stabilized jellium model, *Phys. Rev. B.*, 1999, V. 59, No. 19, pp. 12652–12660.

18. Sarria I., Henriques C., Fiolhais C., Slabs of stabilized jellium: Quantum-size and self-compression effects, *Phys. Rev. B.,* 2000, V. 62, No. 3, pp. 1699–1705.
19. Smogunov A. N., Kurkina L. I., Farberovich O. V., Electronic structure and polarizability of quantum metallic wires, *Phys. Solid State*, 2000, V. 42, pp. 1898–1907.
20. Horowitz C. M., Constantin L. A., Proetto C. R., Position-dependent exact-exchange energy for slabs and semi-infinite jellium, *Phys. Rev. B.,* 2009, V. 80, No. 23, 235101 p.
21. Feibelman P. J., Hamann D. R. Quantum-size effects in work functions of free-standing and adsorbed thin metal films, *Phys. Rev. B.*, 1984, V. 29, No. 3, pp. 6463–6467.
22. Boettger J. C., Persistent quantum-size effect in aluminum films up to twelve atoms thick, *Phys. Rev. B.,* 1996, V. 53, No. 19, pp. 13133–13137.
23. Zhang Z., Niu Q., Shih C.-K., Electronic Growth of Metallic Overlayers on Semiconductor Substrates, *Physical Review Letters*, 1998, V. 80, No. 24, pp. 5381–5384.
24. Kiejna A., Peisert J., Scharoch P. Quantum-size effect in thin Al(110) slabs, *Surface Scienc*e, 1999, V.432, No. 1–2, pp. 54–60.
25. Pogosov V. V., Sum-rules and energy characteristics of small metal particle, Solid State Communications, 1990, V. 75, No. 5, pp. 469–472.
26. Kiejna A., Pogosov V. V. On the temperature dependence of the ionization potential of self-compressed solid- and liquid-metallic clusters, *Journal of Physics: Condensed Matter,* 1996, V. 8, No. 23, pp. 4245–4257.
27. Hirabayashi K., Dielectric theory of the barrier height at metal-semiconductor and metal-insulator interfaces, *Phys. Rev. B.,* 1971, V. 3, No. 12, pp. 4023–4025.
28. Puska M. J., Nieminen R. M., Manninen M., Electronic polarisability of small metal spheres, *Phys. Rev. B*, V. 31, 1985, 3486 p.
29. Rubio A., Serra L., Dielectric screening effects on the photoabsorption cross section of embedded metallic clusters, Phys. Rev. B., 1993, V. 48, No. 24, pp. 18222–18229.
30. Perdew J. P., Tran H. Q., Smith E. D. Stabilized jellium: Structureless pseudopotential model for the cohesive and surface properties of metals, *Phys. Rev. Lett.,* 1990, V. 42, No. 18, pp. 11627–11636.
31. Perdew J.P., Zunger A., Self-interaction correction to density-functional approximations for many-electron systems, *Phys. Rev. B.,* 1981, V. 23, No. 10, pp. 5048–5079.
32. Babich A. V., Pogosov V. V., Effect of dielectric coating on the electron work function and the surface stress of a metal, *Surface Science,* 2009, V. 603, No. 16, pp. 2393–2397.
33. Serena P.A., Soler J.M., Garcia N., Self-consistent image potential in a metal surface, *Phys. Rev. B.,* 1986, V. 34, pp. 6767–6769.
34. Constantin L. A., Pitarke J. M., Adiabatic-connection-fluctuation-dissipation approach to long-range behavior of exchange-correlation energy at metal surfaces: A numerical study for jellium slabs, *Phys. Rev. B.,* 2011, V. 83, No. 7, 075116 p.
35. Lang N. D., Kohn W., Theory of Metal Surfaces: Charge Density and Surface Energy, *Phys. Rev. B.,* 1970, V. 1, 4555 p.
36. Pogosov V. V., On some tenzoemission effects of the small metal particles, *Chem. Phys. Lett.,* 1993, V. 193, 129 p.
37. Pogosov V. V., Kurbatsky V. P., Density-Functional Theory of Elastically Deformed Finite Metallic System: Work Function and Surface Stress*, Journal of Experimental and Theoretical Physics*, 2001, V. 92, No. 2, pp. 304–311.
38. Stampfli P.,Theory for the electron affinity of clusters of rare gas atoms and polar molecules, *Phys.Rep.,* Vol. 255, 1995, pp. 1–77 .
39. Rhoderick E. H., Metal-semiconductor contacts, Clarendon Press, Oxford, 1978, 252 p.
40. Lin L., Li H., Robertson J. Identifying a suitable passivation route for Ge interfaces, *Appl. Phys. Lett.,* 2012, V. 101, 172907 p.
41. Fowler R. H., Nordheim L., Electron Emission in Intense Electric Fields, *Proc. Roy. Soc.*, 1928, A 119, 173 p.
42. Fomenko V. S., Emissiony'e svojstva materialov. Kiev, Naukova dumka, 1981, 339 p.
43. Michaelson H. B., The work function of the elements and its periodicity, *J. Appl. Phys.,* 1977, V. 48, 4729 p.
44. Brewer J. C., Walters R. J., Bell L. D. Determination of energy barrier profiles for high-k dielectric materials utilizing bias-dependent internal photoemission, *Appl. Phys. Lett.,* 2004, V. 85, 4133 p.
45. Singh K., Hammond S.N.A., Current-Voltage Characteristics and Photoresponse of Metal Metal Devices, *Tur. J. of Phys.,* 1998, V. 22. No. 4, 315 p.
46. Moongyu Jang, Junghwan Lee, Analysis of Schottky Barrier Height in Small Contacts Using a Thermionic-Field Emission Model, *ETRI Journal,* 2002, V. 24, No. 6, pp. 455–461.
47. Louie S. G., Cohen M. L., Electronic structure of a metal-semiconductor interface, *Phys. Rev. B,* 1976, 13, 2461 p.
48. Bordier G., Noguera C., Electronic structure of a metal-insulator interface: Towards a theory of nonreactive adhesion, *Phys. Rev. B,* 1991, V. 44, No. 12. pp. 6361–6371.
49. Zavodinsky V. G., Kuyanov I. A., Schottky barrier formation in the Au/Si nanoscale system : A local density approximation study, *J. Appl. Phys.,* 1997, V. 81, No. 6, pp. 2715–2759.
50. Peacock P. W., Robertson J., Band offsets and Schottky barrier heights of high dielectric constant oxides, *J. Appl. Phys.,* 2002, V. 92, pp. 4712–4722.
51. Monch W., Role of virtual gap states and defects in metal-semiconductor contacts, *Phys. Rev. Lett.,* 1987, V. 58, No. 12, pp. 1260–1263.
52. Arponen J., Hautojarvi P., Nieminen R., Charge density and positron annihilation at lattice defects in aluminium, *Journal of Physics F: Metal Physics,* 1973, V. 3, 2092 p.